Supporting Information for "Functional and Structural Models for the Nickel-Iron Hydrogenase"

by Bryan E. Barton and Thomas B. Rauchfuss

Contents:

For the case of hydrogen-evolution catalysis by [**2**H]$^{+}$:[1]

$$\frac{i_c}{i_p} = \frac{n}{0.4463}\sqrt{\frac{RTk}{F\nu}}$$

where n = total number of electrons transfered (2)
R = gas constant (8.31 J mol^{-1} K^{-1})
T = temperature (K)
F = Faraday's constant (9.64853E4 C)
ν = scan rate (V/s)
k = rate constant (s^{-1})

For i_c/i_p = 16 collected at 0.1 V/s, 298 K

16 = (4.4813) * sqrt($RTK/F\nu$)
$(3.57)^2 = RTK/F\nu$
(12.75)*(96485.3*0.1) = (8.31)(298)k
49.67 s^{-1} = k

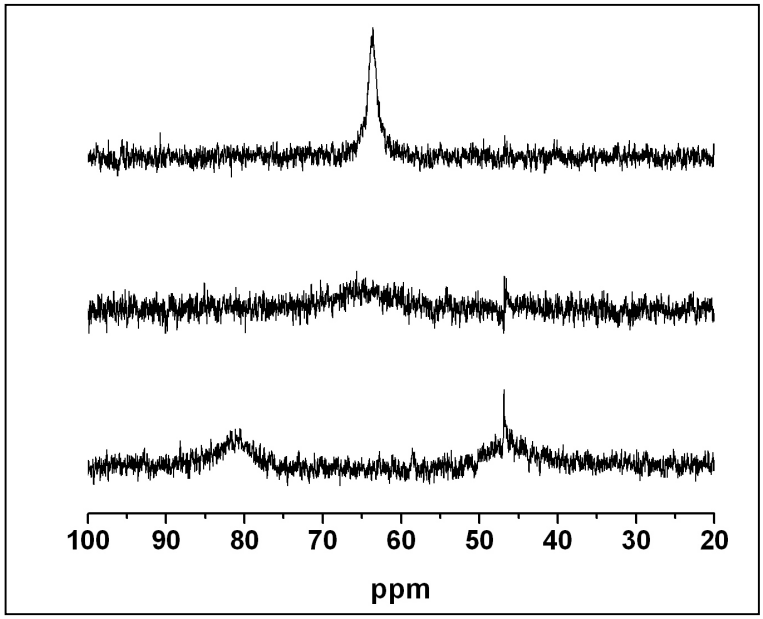

Figure SI-1. Variable temperature $^{31}P\{^{1}H\}$ (161 MHz, CD_2Cl_2) NMR spectrum of **1**. Top: 0 °C; middle: -30°C; bottom -68 °C. At the lowest temperature, most of the sample has precipitated from solution at low temperature, verified by ejecting the NMR sample tube. The signal at δ48 arises from an impurity of $Ni(dppe)_2$.

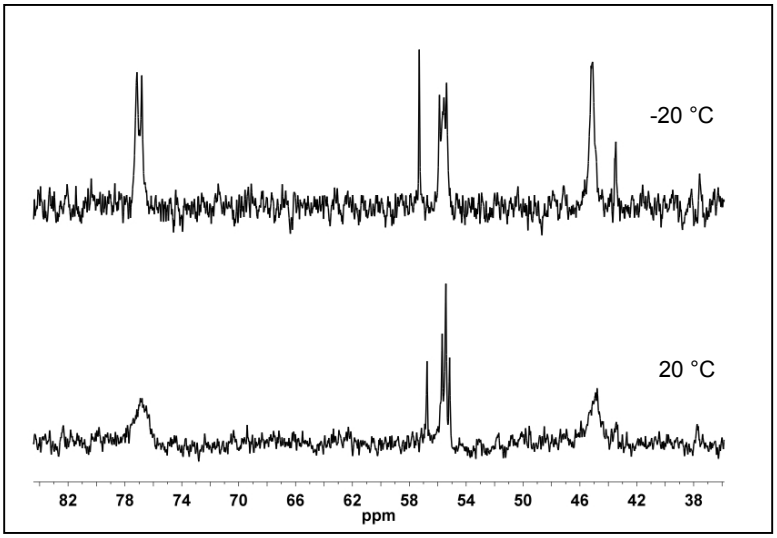

Figure SI-2. $^{31}P\{^{1}H\}$ NMR (161 MHz, CD_2Cl_2) spectrum of **3**. Signals at δ 77 and 45 are assigned to the Ni(dppe) center. The signal at δ 55 is assigned to the $Fe(PPh_3)(CO)_2$ center. Signals at δ 57 and δ 44 are assigned to impurities of Ni(pdt)(dppe) and $Ni(dppe)_2$, respectively. A room temperature spectrum of a cleaner sample of **3** is presented in the main text.

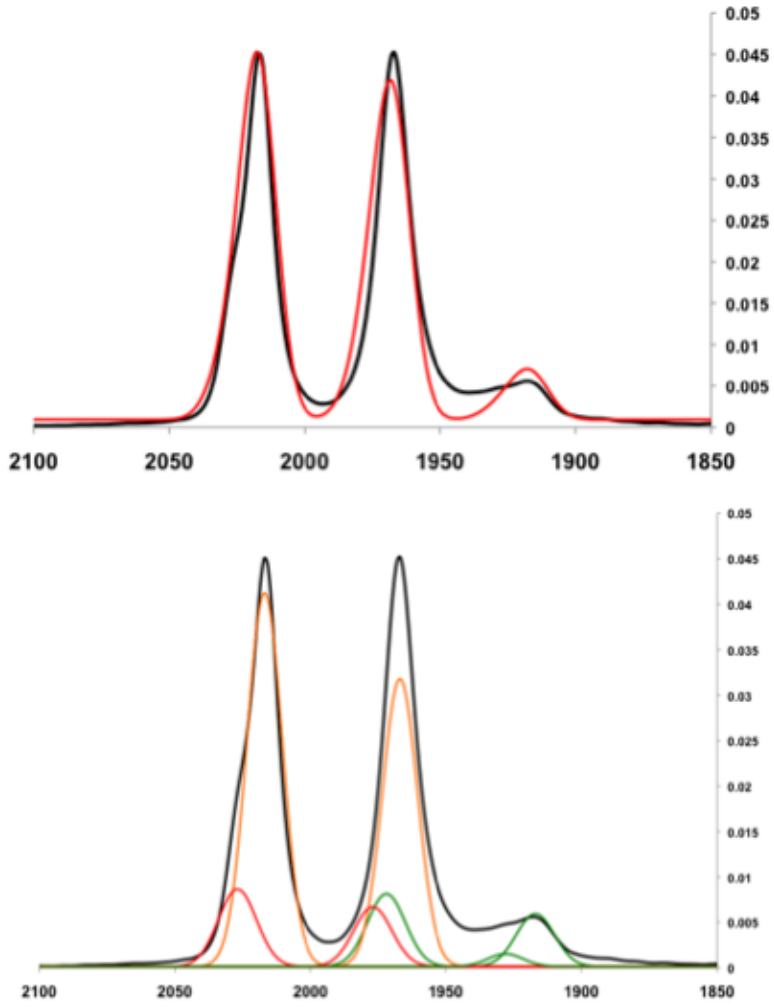

Figure SI-3. Bottom: Observed FT-IR spectrum for [**4**H]$^+$ in THF solution (black), and simulated as containing 15% [**4**H$_2$]$^{2+}$ (red), 70% [**4**H]$^+$ (orange), 15% **4** (green). Simulation parameters for **4** were taken from a fit of **4** in THF (not shown), whereas the spectra for [**4**H]$^+$ and [**4**H$_2$]$^{2+}$ were recorded on acetone and CH_2Cl_2 solutions, respectively.
Top: Observed FT-IR for [**4**H]BF_4 in THF solution (black), and the summation for the simulation (red).

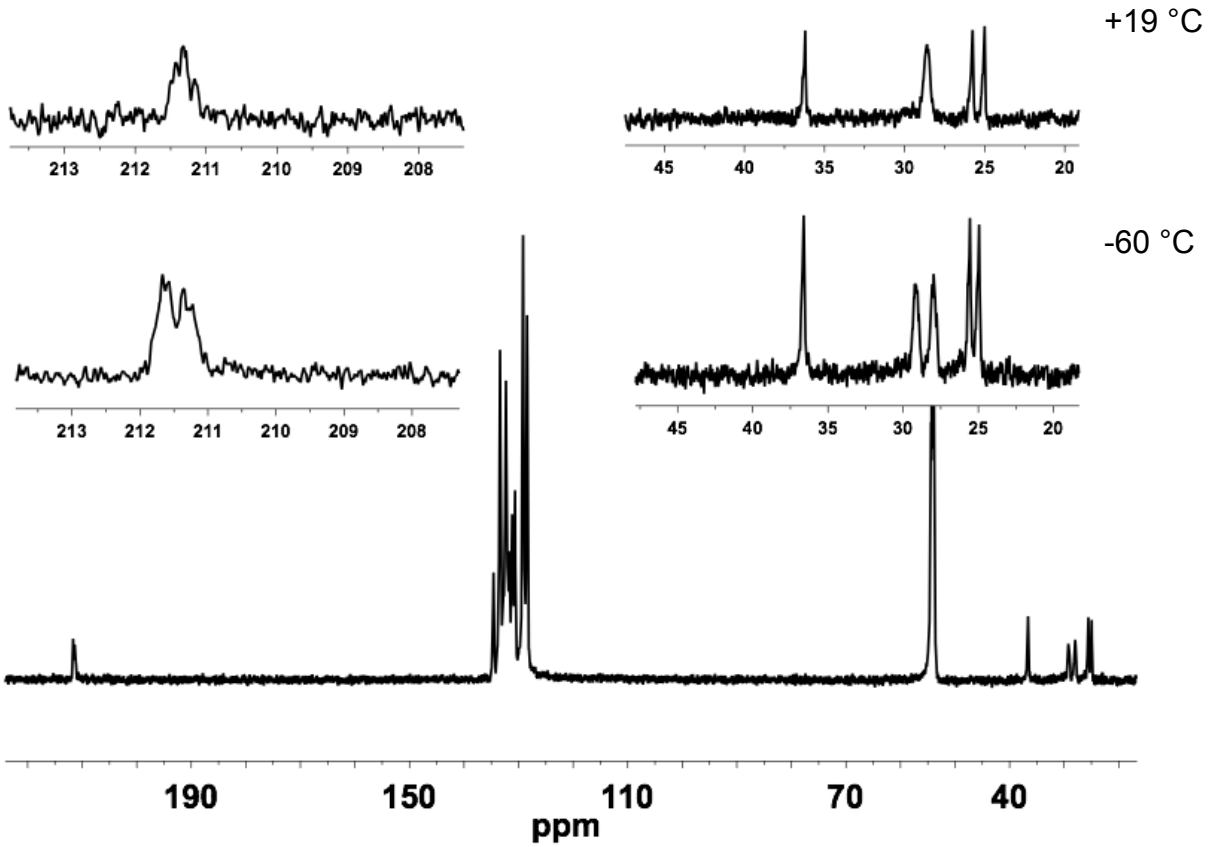

Figure SI-4. $^{13}C\{^{1}H\}$ NMR spectrum (CD_2Cl_2, -60 °C) of [**3**H]BF_4 showing three inequivalent ^{13}C signals for the pdt ligand, two signals for $PPh_2CH_2CH_2PPh_2$, and two signals for $Fe(CO)_2(PPh_3)$, each appearing with discernable $^{2}J_{PC}$. Insets show expanded regions of interest and include corresponding $^{13}C\{^{1}H\}$ NMR spectra at +19 °C, showing that the dppe backbone signals coalesce before the SCH_2N

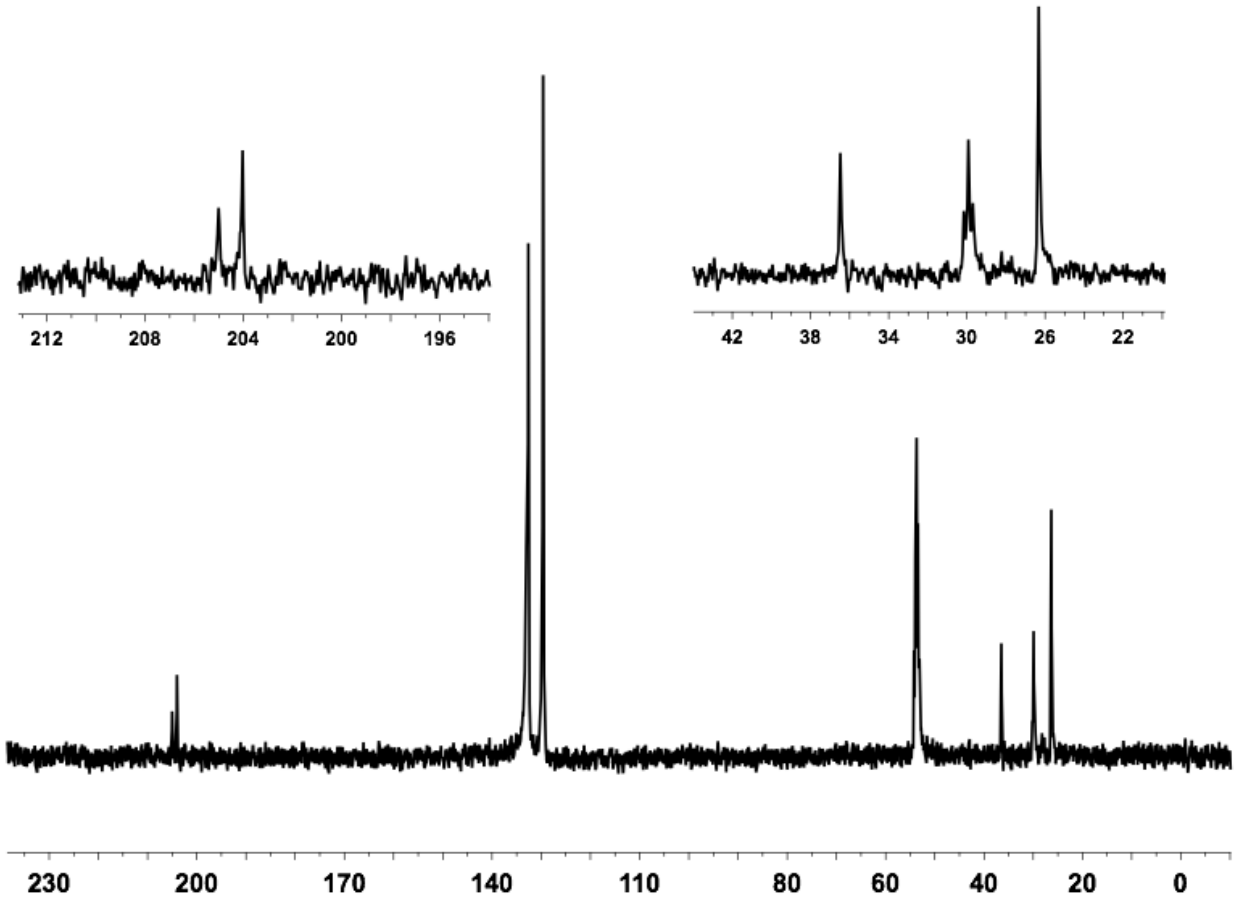

Figure SI-5. $^{13}C\{^{1}H\}$ NMR spectrum (CD_2Cl_2, +19 °C) of [**1**H]BF_4 showing two pdt signals (26, 36 ppm), one $PPh_2CH_2CH_2PPh_2$ signal (*t*, 30 ppm, $^{1}J_{PC}$~$^{2}J_{PC}$), and two $Fe(CO)_3$ signals (204, 205 ppm).

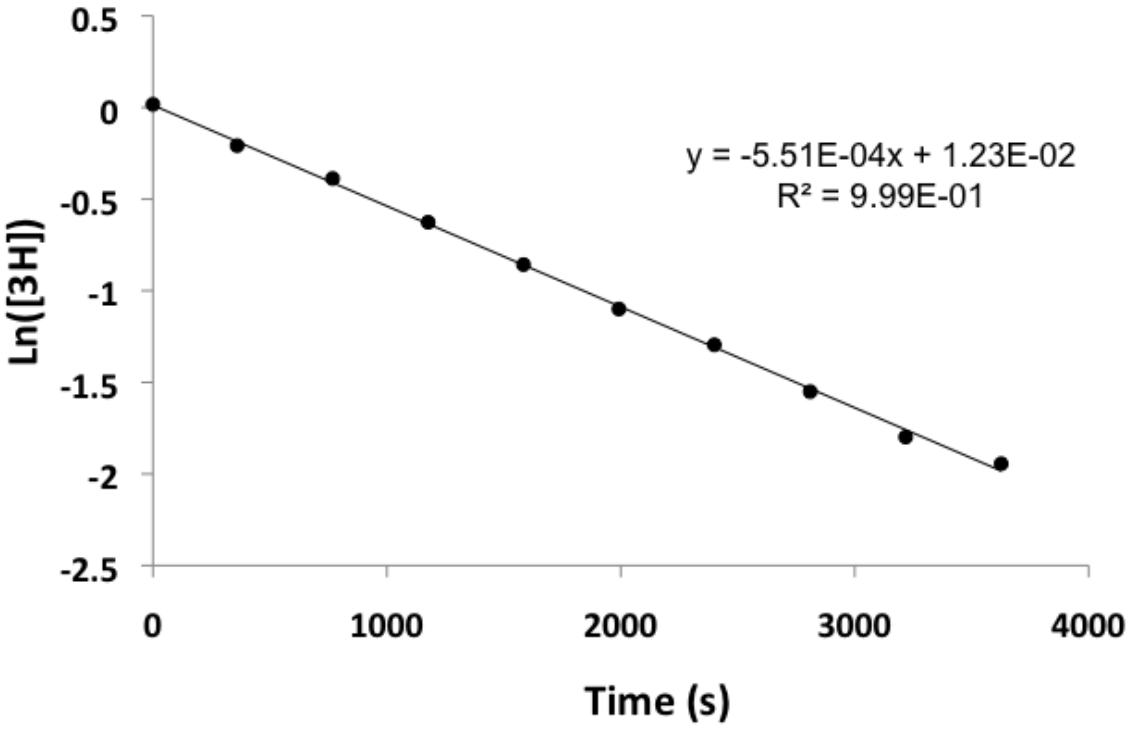

Figure SI-4. Pseudo-first-order H/D exchange kinetics of [**3**H]BF_4 in the presence of excess D_2O in d^6-acetone solution. Concentration of [**3**H]BF_4 was calculated by integration of the hydride signal (δ –3.08) against a normalized phenyl signal. Under these conditions (see Experimental), k = 5.5 x 10^{-4} s^{-1} ($t_{1/2}$ = 21 min).

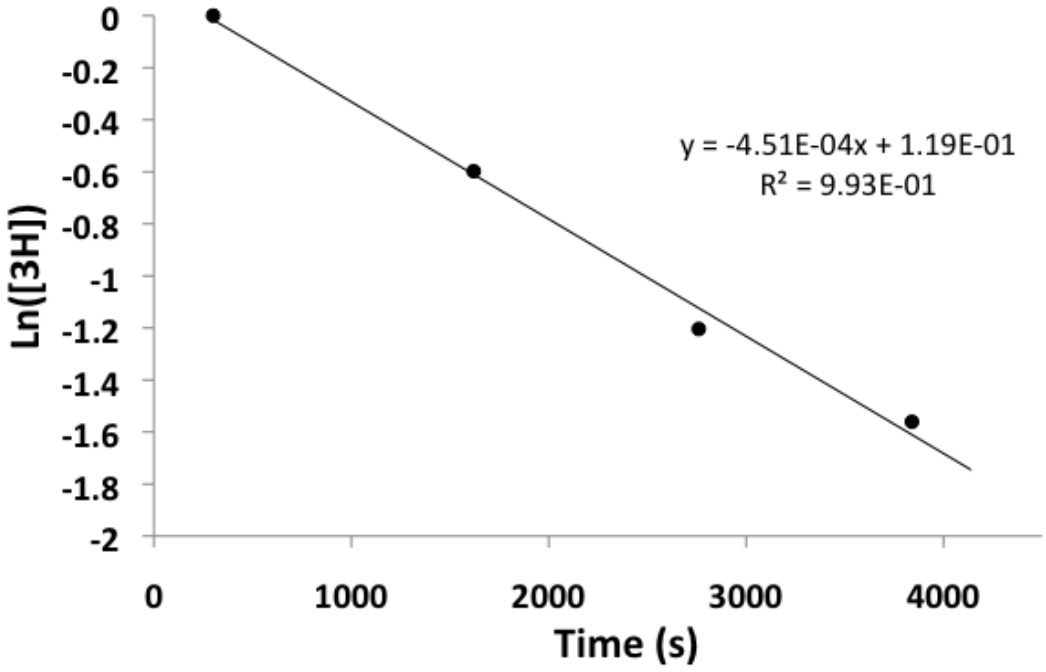

Figure SI-5. Pseudo-first-order decay plot for the reaction of [**3**H]BF_4 with NEt_3 as monitored by $^{31}P\{^1H\}$ NMR spectroscopy. Under these conditions (see Experimental), $k \sim 4.5 \times 10^{-4}$ s^{-1}, $t_{1/2}$ = 28 min).

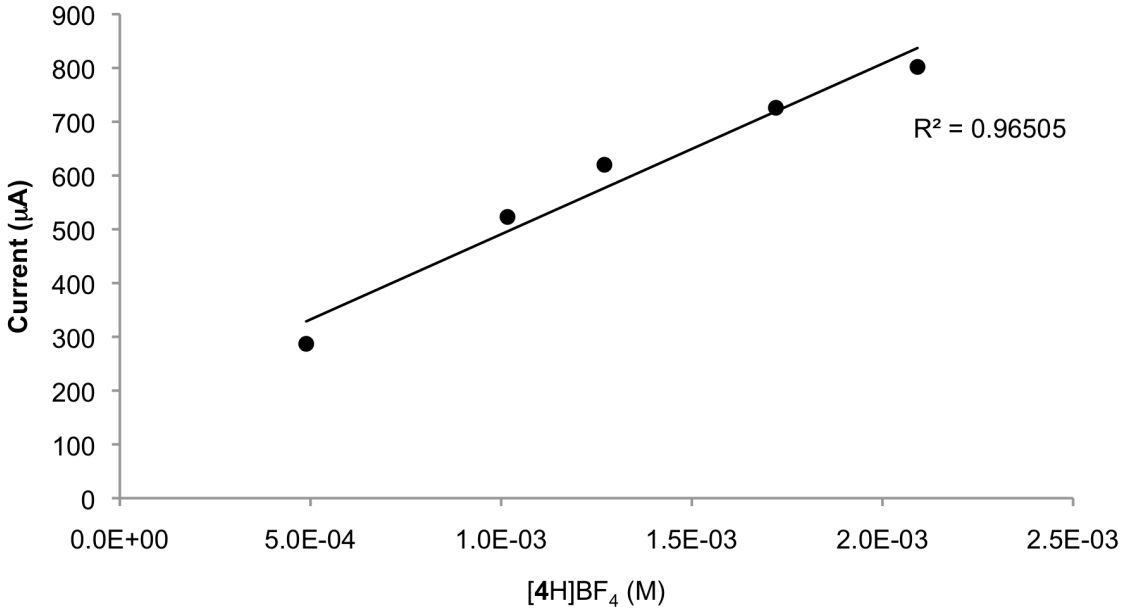

Figure SI-7. Dependence of catalytic current for a 0.389 M solution of CF_3CO_2H vs. concentration of [**4**H]BF_4.

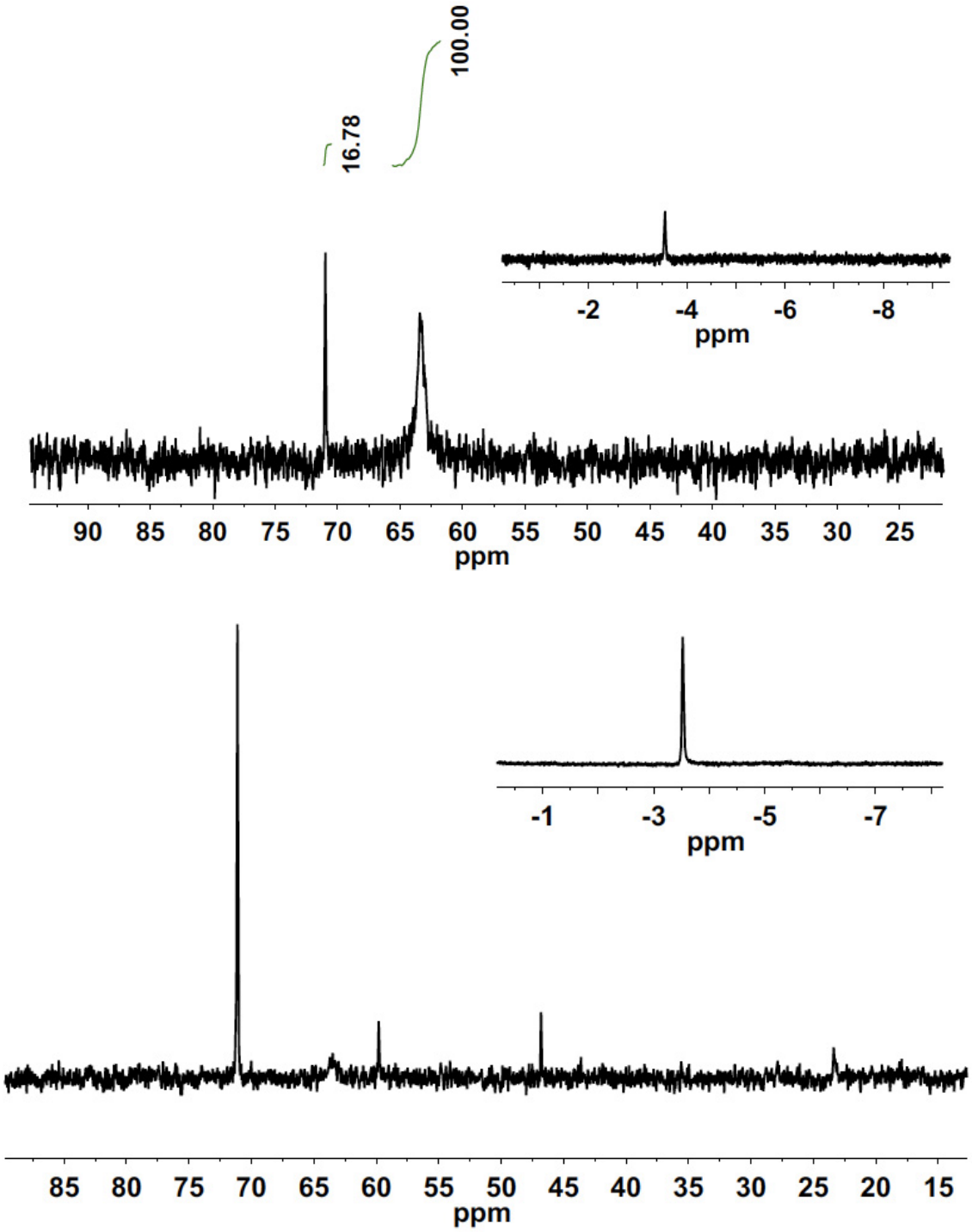

Figure SI-8. Top: $^{31}P\{^{1}H\}$ NMR (202 MHz) of **1** (δ 64) with $B(C_6F_5)_3$ showing a ~16% conversion to the hydride $[\mathbf{1}H]^+$ (δ 71) presumably from the reaction of $B(C_6F_5)_3$ and water from the CD_2Cl_2 ampule. Bottom: $^{31}P\{^{1}H\}$ NMR (202 MHz) of the same NMR tube with H_2 added. Insets: high-field ^{1}H NMR spectra (500 MHz) showing bridging hydride signal.

(1) Fraze, K.; Wilson, A. D.; Appel, A. M.; Rakowski DuBois, M.; DuBois, D. L. *Organometallics* **2007**, *26*, 3918-3924.